Korean J. Chem. Eng., 38(11), 2341-2346 (2021)
DOI: 10.1007/s11814-021-0866-5

pISSN: 0256-1115
eISSN: 1975-7220

Investigation of thermal, antibacterial, antioxidant and antibiofilm properties of PVC/ABS/ZnO nanocomposites for biomedical applications

Muhammad Shabbir Shakir, Muhammad Kaleem Khosa†, Khalid Mahmood Zia, Muhammad Saeed, Tanveer Hussain Bokhari, and Muhammad Abid Zia

Department of Chemistry Government College University Faisalabad 38000, Pakistan
(*Received 3 April 2021 • Revised 24 May 2021 • Accepted 9 June 2021*)

Abstract−The Present study deals with synthesis of PVC/ABS/ZnO nanocomposites with Zinc oxide nanoparticles of particle size less than 50 nm by sonication and solution casting techniques. After characterization, such nanocomposite materials were subjected to thermal study, antibiofilm, antibacterial and antioxidant screening. Nanocomposites films showed higher thermal stability than pure polymer matrix loaded with different ZnO-Nps concentration with homogeneous distribution. Antibacterial studies were carried out against selected gram-positive bacteria: *Staphylococcus aureus* and gram-negative bacteria: *Pseudomonas aeruginosa*. Selective antibiofilm activity was studied against *Staphylococcus aureus* and *Pseudomonas aeruginosa*, which showed a higher to lower activity as a model pathogenic strains (~93 and ~89 at 160 μg/ml concentration, respectively), while free radical scavenging capacity was assessed by DPPH, $ABTH^{+}$ and FRAP methods. PVC/ABS/ZnO nanocomposite showed larger zones of inhibition and higher antibiofilm and antioxidant activity than PVC/ABS polymer matrix. PVC/ABS/ZnO nanocomposite showed enhanced thermal stability and biological properties that qualify them for different biomedical and industrial applications.

Keywords: Nanocomposites, Nanoparticles, Antibacterial, Antioxidants, Antibiofilms

INTRODUCTION

Polymeric nanocomposites are considered the most attractive class of materials owing to their versatile properties by using low to high content in nano forms [1,2]. Addition of inorganic nanoparticles (NPs) to polymers matrix may present promising functionalities like antibacterial, catalytic activity, in addition to developing mechanical, electrical properties, thermal stability, and fire retardancy [3-5]. A variety of nanoparticle (NPs) reinforced composites have been developed that typically consist of up to 5% w/w NPs [6]. The addition of NPs into films has made end-products fire resistant, lightweight, stronger in thermal and mechanical performance and less permeable to moisture and gases. When incorporated in plastic films, nanoparticles, such as zinc oxide (ZnO) and silica and titanium dioxide (TiO_2), are capable of reducing the flow of oxygen inside packaging containers. They also act as a barrier against moisture to keep food fresh for an extended period [7].

Nowadays, Zinc oxide nanoparticles have attained much attention because of their potential applications in biomedical and industrial fields [8-10]. The extensive use of available antimicrobial drugs is the main cause of resistance against new bacterial strains and non-respondent to existing antibiotics. Furthermore, excessive production of reactive radicals or their precursors in bio-systems are the cause of many diseases like arthritis, cardiovascular, diabetes and cancer [11,12]. The antibacterial properties of ZnO-Nps were investigated against both Gram-positive and Gram-negative bacteria. During bactericidal activity study, various properties (e.g., particle size, solubility, surface area) of ZnO samples were maintained unaltered when varying the others [13]. Orthopedic implant surfaces provide suitable conditions for bacterial infection. As a result, biofilm formation is one of the most serious complications of implant surgery, biofilm is a multicellular aggregation of bacteria covered with a hydrated extracellular polymeric matrix of their own synthesis and characterized by cells that are permanently attached to an interface with each other. Antibiotic susceptibility of bacteria embedded with a biofilm is less as a result, treatment requires higher doses of therapeutic agents. Therefore, the treatment of implant-associated infection using antibiotics fails to clear the pathogens. Revision surgery is often the only viable option [14], In biological systems, production of highly reactive radical species or their precursors leads to oxidative stress, which has been observed in various diseases such as cancer, cardiovascular disease, diabetes, and arthritis [15]. Antioxidants play an important role in the functioning of all biosystems. Antioxidant and free radical scavenging activity of ZnO-Nps in biological systems have been described [16]. For this purpose, there is a great need to find effective antimicrobial drugs. Nanocomposite materials have been proposed as an alternative to overcome such issues. So the antioxidants are important for functioning of all bio-systems [17-19]. To extend the scope of our research work, we emphasized the influence of ZnO-Nps to the PVC/ABS blend in in-situ emulsion polymerization. Initially, the hydrothermal method was used to fabricate ZnO-Nps. Nanocomposite films were synthesized by loading the different weight ratio of prepared ZnO-Nps to PVC/ABS (80 : 20) blend. After characterization, such nanocomposites were subjected to study their thermal, antibacterial, selective antibiofilm and antioxidant properties.

†To whom correspondence should be addressed.
E-mail: mkhosapk@yahoo.com

MATERIALS AND METHODS

1. Chemicals

Polyvinyl chloride (PVC, Mw.48000 D), acrylonitrile-butadiene styrene (ABS), Zinc acetate, Hydrogen peroxide, Methanol, DPPH, ABTH, THF and DMSO were purchased from analytical Sigma Aldrich and used as such without further purification.

2. Instrumental Techniques

The FT-IR spectrophotometer (Bruker) was used for the confirmation of functional groups in synthesized PVC/ABS/ZnO nanocomposite and the spectra were recorded between the range 4,000 to 400 cm^{-1}. Thermal stability of ternary nanocomposites was determined by DSC 404 C Netzsch and Perkin Elmer TGA-7 under nitrogen atmosphere at the rate of 10 °C min^{-1} from room temperature to 700 °C in terms of temperature (T_5 %), (T_{10} %) and (T_{max}). Antibiofilm activity was determined by using Microplate Reader (ELx808^{TM} Absorbance, Biotek, USA).

3. Fabrication of Zinc Oxide Nanoparticles

The hydrothermal method was used to fabricate ZnO-Nps with particle size less than 50 nm in alcoholic medium by the reaction of zinc acetate and H_2O_2. Typically, 5 gm zinc acetate was dissolved in 250 ml of DI water Subsequently, methanol (300 ml), hydrogen peroxide H_2O_2 (4 mL, 47%) were added slowly while stirring to get a clear solution. The resulting clear solution was heated at 80 °C with stirring for 2 hr. After that, the NaOH (0.1 M) solution was added dropwise to get white precipitate of ZnO-Nps. The powder zinc oxide-Nps were dried at 80 °C in a drying oven then calcinated at 600 °C for 1 h [20].

4. Synthesis of PVC/ABS/ZnO-nanocomposite

PVC/ABS/ZnO-nanocomposites were synthesized by sonication and solution casting technique [21]. Typically, PVC/ABS (80 : 20 wt%) was dissolved in dry THF by stirring at room temperature for about 24 hrs. Zinc oxide-NPs with different weight ratio (1, 2.5, 5, 7.5 and 10%) were added to PVC/ABS blend and heated gently with stirring to get a homogeneous mixture, which was cast onto glass plates and kept in air to dry for further characterization and study.

5. Moisture Absorption Studies

The moisture uptake ability of nanocomposite materials depends on the chemical structure of the matrix as well as size of nanoparticles and is responsible for changing the dielectric constant. Moisture absorption capability of synthesized PVC/ABS blend with different contents of ZnO-Nps was calculated by the changes in weight of ternary nanocomposite before and after immersion in deionized water for 24 hrs. at room temperature. The % of water uptake was found as follows:

$$(\%\ \text{Water absorption})\ WA = \frac{W - W_0}{W_0} \times 100$$

where W and W_0 are the weight of the nanocomposite before and after immersion.

ANTIBACTERIAL ASSAY

Synthesized ternary composites (PVC/ABS/ZnO-Nps) were subjected to investigate the antibacterial activity against six bacterial strains: *S. aureus*, *B. subtilis* and *S. pyogenes* (Gram-positive) and *P. aeruginosa*, *E. coli* and *S. Typhi* (Gram-negative) by disc-diffusion method [22,23]. The strains were cultured at 37 °C in nutrient broth for 24 hrs. The broth culture of test organisms of approximately 10^4-10^6 (CFU/mL) was added to agar medium into sterile petri dishes at 45 °C and let stand to solidify. Solution of ternary composite in DMSO (15 μL) was poured on sterile paper disks and such paper disks were placed on nutrient agar plates. Triplicate plates of each organism were prepared and incubated at 37 °C for 24 hrs. In each plate Cefixime (1 mg/mL) served as a reference antibacterial drug, Finally, the diameter of the zone of inhibition in (mm) was measured and compared with standard antibiotic drug. The antimicrobial activity of the tested samples was evaluated by diameter of zone of inhibition; the larger the diameter of zone of inhibition, the greater will be the ability of polymer blend to resist bacteria.

ANTIBIOFILM ACTIVITY

The ability of PVC/ABS/ZnO nanocomposites to inhibit the formation of biofilm was tested against selected gram-positive bacteria: *Staphylococcus aureus* and gram-negative bacteria: *Pseudomonas aeruginosa* which showed a higher to lower activity as a model pathogenic strains. The selective biofilm forming bacteria were grown in 10 ml of tryptic soy broth (TSB) with 1% glucose at 37 °C for 24 hrs. Each diluted bacterium (200 μL) was inoculated into 96 well microliter plates containing synthesized ternary nanocomposite. The plates were further incubated at 37 °C for 24 hr; after incubation, each well was washed with saline phosphate buffer of pH 7.2 and dried at room temperature for half an hour. On drying, a solution of crystal violet (200 μL of 0.1% w/v) was added. Finally, 100 μL of 96% ethanol was added to each well to extract stained bound biofilm and left for further 30 min. Absorbance of crystal violet was measured at 490 nm with the help of Microplate Reader. Inhibition in biofilm was measured and compared with control [24]. Ciprofloxacin was used as positive control (20 μg ml^{-1}) as a biofilm inhibitor. The percentage of inhibition of biofilm formation was calculated by using the following equation:

$$\%\ \text{of inhibition} = 1 - \left(\frac{\text{optical density of composite}}{\text{optical density of negative control}}\right) \times 100$$

ANTIOXIDANT ASSAYS

1. DPPH Free Radical Scavenging Assay

DPPH (1,1-diphenyl-2-picrylhydrazyl) free radical inhibition activity of ternary composites (PVC/ABS/ZnO-Nps) was determined according to standard reported method [25]. Briefly, 3 mL of 100 μM DPPH solution in methanol was added to 1 mL of PVC/ABS blend as well as PVC/ABS/ZnO nanocomposite solution in methanol, concentration of (50, 100, 150, 200, 300 and 400 μg/mL) by sonication. After sonication, the solution was kept in a dark chamber at 37 °C for 30 minutes. The color of DPPH changed from deep-violet to light-yellow and absorbance was noted on the spectrophotometer (Agilent 8453) at 517 nm. The ascorbic acid served as a reference.

The percentage scavenging activity was calculated by applying

the following formula:

$$\% \text{ scavenging activity} = \frac{\text{absorbance of control} - \text{absorbance of test sample}}{\text{absorbance of control}} \times 100$$

2. $ABTH^{+}$ Radical-scavenging Activity

The ABTH (2,2-azino-bis-(3-ethylbenzothiazoline-6-sulfonic acid) scavenging activity of the PVC/ABS blend loaded with different concentrations (1, 2.5, 5.0, 7.5 and 10%) of ZnO-Nps was investigated as per reported method with some modification [26]. The solution of ABTH in methanol (7 mM) and potassium persulfate (2.45 mM) solution were mixed and kept in a dark chamber at room temperature for 16 hrs, and the absorbance was noted at 734 nm. Similarly, in another vial, a mixture of nanocomposite (100 μL) and ABTH (1,900 μL) was kept in the dark chamber at ambient temperature for 2 hrs. The absorbance was noted at 734 nm by a microplate reader. The (%) of $ABTH^{+}$ free radical scavenging activity was calculated as follows:

$$\% \text{ scavenging activity} = \frac{\text{absorbance of blank} - \text{absorbance of test nanocomposite}}{\text{absorbance of blank}} \times 100$$

3. Ferric-reducing Antioxidant Potential (FRAP)

The ferric reducing-antioxidant power (FRAP) was determined according to the reported method [27]. Typically, ferric-reducing antioxidant potential (FRAP) reagent was prepared by mixing $FeCl_3$ (20 mM) solution, tripyridyl-s-triazine (10 mM) (TPTZ), and acetate buffer of pH 3.6 (300 mM) with a 1 : 1 : 10 ratio. FRAP reagent (200 μL) was added to the synthesized nanocomposite solution (100 μL) prepared by sonication. The mixture was incubated at room temperature for 2 hrs and absorbance was noted at 590 nm. Ferrous sulfate ($FeSO_4$) was used as a control to find the concentration of ferric reducing-antioxidant power, which was expressed as mg of ferrous sulfate ($FeSO_4$) equivalent per gram dry weight of nanocomposite material.

RESULTS AND DISCUSSION

1. Physicochemical Properties of PVC/ABS/ZnO-nanocomposites

Fig. 1 shows the FT-IR absorption spectra of PVC/ABS polymer matrix with 10% (w/w) concentrations of Zinc oxide nanoparticles. The absorption spectrum of pure PVC showed characteristic absorption bands at 2,919, 2,821 cm^{-1} for (-CH) and (-CH_2) asymmetric stretching, while the bands at 1,425, 1,329, 1,252, 957 and 610 cm^{-1} were attributed to (-CH) bending, respectively. Pure ABS showed an IR absorption band at 697 cm^{-1} attributed to -CH_2 rocking vibration; the band at 2,237 cm^{-1} is associated with the nitrile functional group, characteristic of acrylonitrile in ABS and absent in this region for PVC. In PVC/ABS blend, there is absence of a peak in the region of 1,400 to 1,200 cm^{-1} in the IR spectrum for PVC and increase in intensity of the peak at 2,237 cm^{-1}, confirming the interaction of polar functional groups of PVC and ABS, acrylonitrile group of ABS with the C-H group of PVC. While in PVC/ABS/ZnO nanocomposite with 10% (w/w) ZnO-Nps, the small band at 1,466 cm^{-1} disappeared and the intensity of sharp bands at 1,682 cm^{-1}, 1,141 and 761 cm^{-1} decreased [28]. A new weak band at 450-700 cm^{-1} for Zn-O and the absorption band of bending O-H group at 1,642 cm^{-1} was observed, which may be due to the complexation between polymeric matrix and the ZnO-Nps which act as a filler. Whereas the sharp band in the range between 700-500 cm^{-1} increased, which may be due to the interaction of functional groups inside the PVC/ABS and Zn^{2+} ions. Such results are consistent with literature values [29]. Moisture absorption capability of nanocomposite materials is directly related to the dielectric constant of composite materials. Those materials having lower moisture uptake value and higher value of dielectric constant have great attraction in microelectronic industries. Moisture absorption capability of PVC/ABS blend gradually decreased by increasing the content of ZnO-Nps (Table 1).

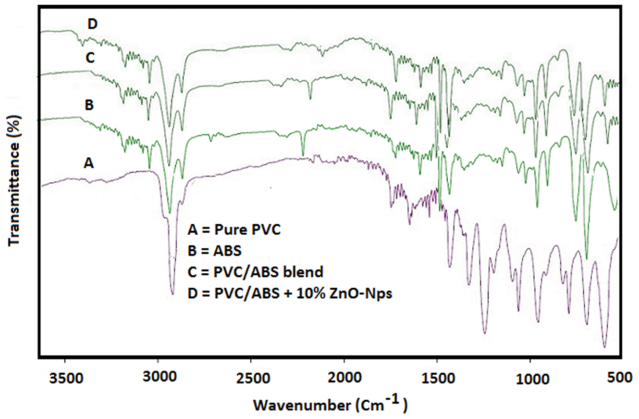

Fig. 1. FT-IR spectra of PVC/ABS blend and blend with 10% ZnO-Nps.

Thermal stability of ternary composite (PVC/ABS/ZnO-Nps) was

Table 1. TGA results and moisture capability of PVC/ABS with different content of ZnO-Nps

ZnO-Nps (%)	PVC/ABS	T_5 °C	T_{10} °C	T_{max}	Char yield (%)	Activation energy (KJ/mol)	Moisture absorption (%)
0	80 : 20	240	265	610	10	128.75	0.61
1		250	270	630	14	110.31	0.58
2.5		255	274	633	16	98.74	0.56
5		260	278	635	16	91.63	0.51
7.5		264	282	644	18	86.25	0.50
10		270	285	650	18	74.46	0.48

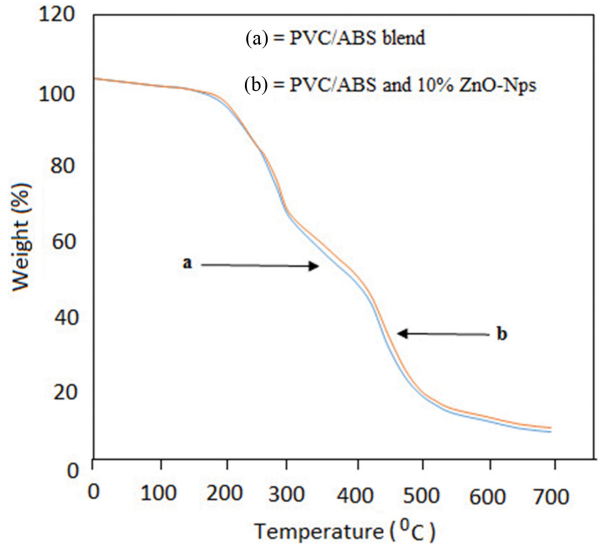

Fig. 2. TGA of (a) PVC/ABS blend (b) PVC/ABS+10% ZnO-Nps.

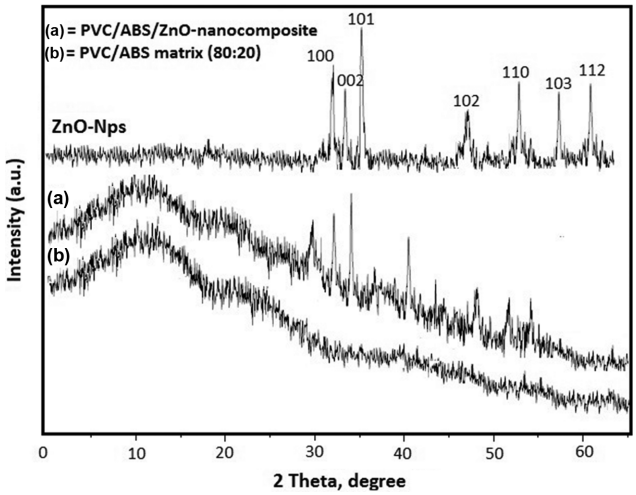

Fig. 3. XRD pattern of PVC/ABS/ZnO nanocomposite.

investigated and data is presented in Table 1. The degradation of nanocomposites with respect to weight loss was observed into three stages (Fig. 2) Initially, total of 10% physically weak and chemically strongly bound H_2O, secondly substantial weight loss about 20-93% attributed the main degradation of blend within the temperature range starts from 240 °C up to 450 °C. After 450 °C, weight loss of the blend occurred sharply due to breakage of backbone of organic matrix. The degradation peaks of the cross-linked polymer were less intense and shifted to higher temperature by increasing the weight ratio content of zinc oxide-Nps. It is clear that the degradation temperature gradually increases with increasing content of ZnO-Nps and the thermal decomposition of all samples shifts slightly toward higher temperature ranges than in the pure PVC/ABS polymer blend, showing the increase of the thermal stability of the prepared nanocomposites. Furthermore, the final weight loss of the pure PVC/ABS blend is less than the PVC/ABS/ZnO nanocomposites; that may be due to the chemical reaction between ZnO-Nps and the active sites of PVC/ABS blend, which increases their thermal stability. From thermal data, energy of activation was calculated by using the Coats and Redfern equation [30]. We found that the activation energy of nanocomposites decreased from 128.75-74.46 KJ/mol by increasing content of ZnO-Nps, which prominently affected the stability of PVC/ABS polymer blend.

2. X-ray Diffraction Pattern

XRD pattern of ZnO nanoparticles is given in Fig. 3. Different peaks are observed at (2θ)=31.85° (1 0 0), 33.55° (0 0 2), 36.75° (1 0 1), 47.65° (1 0 2), 56.75° (1 1 0), 62.95° (1 0 3) and 68.10° (1 1 2), which is in good agreement with the JCPDS data for a typical wurtzite type crystal [25]. The presence of (1 0 0), (0 0 2), (1 0 1) planes in XRD indicates the formation of pure wurtzite structure of ZnO nanoparticles. The X-ray diffraction results and the average crystallite size value were calculated by the Scherer equation; the average crystalline size was found to be 45 nm. Moreover, the XRD pattern illustrated in (Fig. 3(a) and (b)) exhibited the uniform dispersion of ZnO-Nps into the polymer matrix, indicating the ability of PVC/ABS to act as excellent hosts for ZnO-Nps encapsulation. Additionally, the intensity of ZnO-NPs peaks was increased by increasing the content of ZnO-Nps in the PVC/ABS polymer matrix [31].

3. Antibacterial Activity

The mechanism of antibacterial activity of zinc oxide-Nps is still

Table 2. Antibacterial activity of the PVC/ABS blend with different contents of ZnO-Nps

Test compounds	Zone of Inhibition of Sample (mm)±SD					
	S. aureus	*S. pyogenes*	*B. subtilis*	*E. coli*	*S. typhi*	*P. aeruginosa*
PVC/ABS blend	20±1	15±1.5	20±1	15±1	14±1.15	-
Blend+1% ZnO-Nps	21±1.25	18±1.25	22±1.15	16±1.50	16±1.35	-
Blend+2.5% ZnO-Nps	25±1.5	21±1.15	25±1.25	18±1.15	19±1.00	-
Blend+5% ZnO-Nps	27±1.15	24±1.25	27±1.0	19±1.50	20±1.25	14±1.00
Blend+7.5% ZnO-Nps	28±1.0	27±1.0	28±1.15	20±1.25	22±1.15	17±1.5
Blend+10% ZnO-Nps	32±1.25	29±1.15	31±1.25	21±1.15	23±1.0	18±1.0
Cefixime (Standard drug)	33±1.5	31±1.0	35±1	29±0.5	36±1	31±2

±=SD, standard deviation, ($P<0.05$ vs. control)

(5-10 mm zone of inhibition)=Activity present, (11-25 mm zone of inhibition)=Moderate activity, (26-40 mm zone of inhibition)=Strong activity

Table 3. Antioxidant properties of PVC/ABS composite with varying contents of ZnO-Nps

Name of test compounds	Antioxidant activity±SD		
	DPPH assay (%)	ABTS assay (%)	FRAP assay (%)
PVC/ABS blend	45±1.0	24±2.01	0.09±1.50
Blend+1% ZnO-Nps	56±1.5	28±2.25	0.19±1.25
Blend+2.5% ZnO-Nps	64±2.5	35±0.00	0.75±2.50
Blend+5% ZnO-Nps	71±1.5	54±1.50	0.81±2.15
Blend+7.5% ZnO-Nps	77±2.0	61±1.25	0.88±1.15
Blend+10% ZnO-Nps	84±1.0	73±2.10	0.96±1.50

±=SD, standard deviation, (P<0.05 vs. control)

under investigation, but it has been proposed that it may be due to antimicrobial metal ion released and oxidative or non-oxidative stress induction, which may interact with bacterial strains and ultimately damage the bacterial cell wall [32]. Nanocomposites showed stronger antibacterial activity against Gram-positive bacteria compared to Gram-negative bacteria due to the difference in their cell wall structure [33], where lipopolysaccharides present in the Gram-negative bacteria cell wall can block some antimicrobial agents from passing or attaching to cell wall, thereby preventing bacterial cell death [13]. Several studies have shown that zinc oxide-Nps have a wide range of antibacterial activiy against both gram-positive bacteria and gram-negative [34]. PVC/ABS blend loaded with different concentrations of zinc oxide-Nps showed promising activity against all tested gram-positive and gram-negative bacterial strains and results are shown in Table 2. Results show that *Staphylococcus aureus* exhibited higher sensitivity with 10% ZnO-Nps of (32 mm) inhibition zone, while *Pseudomonas aeruginosa* showed poor sensitivity with (18 mm) zone of inhibition, which implies that gram-positive bacteria showed more resistance to increased concentration of ZnO-Nps in PVC/ABS blend, and such results also resemble literature values. It may be due to size, shape, chemical composition and homogeneous mixing of nanoparticles in polymeric matrix and may have a greater effect on their bioactivity inside the cell membrane and cytoplasm. It is also observed from the results that the smaller size of nanoparticles enhanced the efficacy in inhibiting bacterial growth [35].

4. Antioxidant Activity

The antioxidant property of PVC/ABS blend loaded with varying concentration of ZnO-Nps was determined through DPPH·, $ABTH^{+}$, and FRAP assays. and data is presented in Table 3. The free radical scavenging activity by DPPH· radical scavenging assay is 45%, 56%, 64%, 71%, 77% and 84%; $ABTH^{+}$ scavenging assay: 24%, 28%, 35%, 54%, 61% and 73%; and FRAP assay: 0.09%, 0.19%, 0.75%, 0.81%, 0.88% and 0.96% for 1%, 2.5%, 5%, 7.5% and 10% ZnO-Nps loaded PVC/ABS blend, respectively. Results show that inhibition of free radical activity of PVC/ABS/ZnO nanocomposites increased with increasing content of ZnO-Nps.

5. Antibiofilm Activity

Antibiofilm activity of PVC/ABS composites loaded with ZnO-Nps was tested against selected gram-positive bacteria - *Staphylococcus aureus* and gram-negative bacteria - *Pseudomonas aeruginosa* as model microorganisms. PVC/ABS blend showed less antibiofilm activity against biofilm forming bacteria; however, PVC/ABS

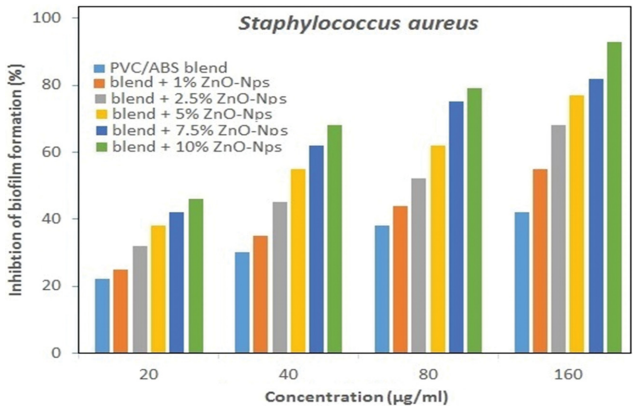

Fig. 4. Antibiofilm activity of PVC/ABS blend with different concentration of ZnO-Nps (P<0.05 vs. control).

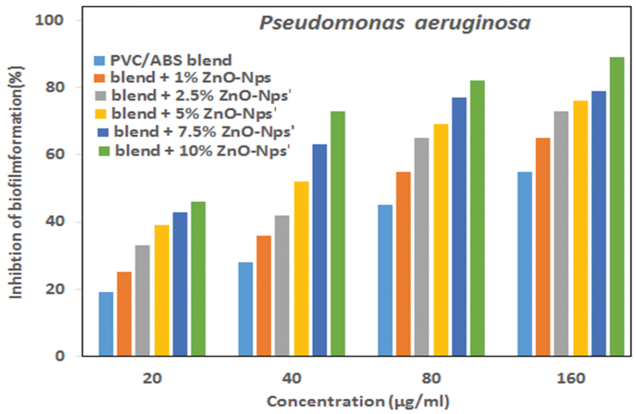

Fig. 5. Antibiofilm activity of PVC/ABS blend with different concentration of ZnO-Nps (P<0.05 vs. control).

blend containing varying content of ZnO-Nps showed good activity. Figs. 4 and 5 show the biofilm formed by tested bacterial strains after treatment with PVC/ABS blend with varying concentration of ZnO-Nps, which showed that inhibition effect is concentration dependent of ZnO-Nps. The continuous release of ZnO-NPs from PVC/ABS/ZnO nanocomposites can explain their antibiofilm activity, where they inhibit exopolysaccharide synthesis, which represents the bacterial main defense system in biofilm forming bacteria [36]. The inhibition perecentage of biofilm formation for *Staphylococ-*

cus aureus and *Pseudomonas aeruginosa* was ~93 and ~89, respectively, at 160 μg/ml concentration of each concentration of nanocomposite materials. From these result, it is clear that the ZnO-Nps containing composite materials showed higher biofilm inhibition activity than PVC/ABS blend. Furthermore, ZnO-Nps concentration in nanocomposites plays an important role in biofilm inhibition percentage where it is directly proportional to antibiofilm activity [37].

CONCLUSION

PVC/ABS/ZnO nanocomposite films were synthesized by sonication and solution casting techniques. PVC/ABS/ZnO nanocomposite showed higher thermal stability than pure PVC/ABS polymer matrix due to homogeneous dispersion through PVC/ABS matrix, preventing the nanoparticles from aggregation. Antibacterial studies were carried out against selected gram-positive bacteria: *Staphylococcus aureus* and gram-negative bacteria: *Pseudomonas aeruginosa.* Selective antibiofilm activity was studied against *Staphylococcus aureus* and *Pseudomonas aeruginosa*, which showed a higher to lower activity as a model pathogenic strains (~93 and ~89 at 160 μg/ml concentration, respectively), while free radical scavenging capacity was assessed by DPPH, $ABTH^{+}$ and FRAP methods. PVC/ABS/ZnO nanocomposite showed larger zones of inhibition and higher antibiofilm and antioxidant activity than PVC/ABS polymer matrix. PVC/ABS/ZnO nanocomposite showed enhanced thermal stability and biological properties that qualify them for different biomedical and industrial applications.

REFERENCES

1. A. M. Youssef, M. E. El-Naggar, F. M. Malhat and H. M. El Sharkawi, *J. Clean Product.*, **206**, 315 (2019).
2. A. M. Youssef and S. M. El-Sayed, *Carbohyd. Polym.*, **193**, 19 (2018).
3. A. M. Youssef, S. M. El-Sayed, H. S. El-Sayed, H. H. Salama, F. M. Assem and M. H. Abd El-Salam, *Int. J. Biol. Macromol.*, **115**, 1002 (2018).
4. M. Youssef and M. T. Nour, *RSC Adv.*, **6**, 36467 (2016).
5. A. W. Hu and Z. H. Fu, *Pack. Eng.*, **24**, 22 (2003).
6. A. Llorens, E. Lloret, P. A. Picouet, R. Trbojevich and A. Fernandez, *Trends. Food Sci. Technol.*, **24**, 19 (2012).
7. Y. Huang, L. Mei, X. Chen and Q Wang, *Nanomaterials*, **8**, 830 (2018).
8. D. Das, B. Chandra, P. Phukon and S. Kumar, *Colloids Surf. B Biointerf.*, **111**, 556 (2013).
9. A. Kumar, K. Sharma and A. R. Dixit, *J. Mat. Sci.*, **54**, 5992 (2019).
10. A. Kumar, K. Sharma and A. R. Dixit, *Med. Hypotheses*, **144**, 110253 (2020).
11. L. Wang, C. Hu and L. Shao, *Int. J. Nanomedicine*, **12**, 1227 (2017).
12. K. M. Nash and S. Ahmed, *Nanomedicine*, **11**, 2033 (2015).
13. M. A. Omnia, K. Z. EL-Baghdady, M. H. K. Mostafa, M. I. El Borhamy and G. A. Meligi, *J. Polym. Res.*, **27**, 74 (2020).
14. Z. Beyenea and R. Ghosh, *Mater. Today Commun.*, **21**, 100612 (2019).
15. S. Ghosh, R. G. Sankar and V. Vandana, *J. Nanosci.*, **2014**, 1 (2014).
16. K. M. Nash and S. Ahmed, *Nanomedicine*, **11**, 2033 (2015).
17. T. Safawo, B. V. Sandeepa, S. Polaa and A. Tadess, *Open Nano*, **3**, 56 (2018).
18. M. S. Shakir, M. K. Khosa, K. M. Zia, M. J. Saif and T. H. Bokhari, *J. Serb. Chem. Soc.*, **86**, 1 (2021).
19. I. Zgura, N. Preda, M. Enculescu, L. Diamandescu, C. Negrila, M. Bacalum, C. Ungureanu and M. E. B. Patrascu, *Materials*, **13**, 182 (2020).
20. V. Doddapaneni, M. Saleemi, F. Ye, R. Gati and M. S. Toprak, *Compos. Sci. Technol.*, **141**, 113 (2017).
21. S. Hammani, A. Barhoum and M. Bechelany, *J. Mater. Sci.*, **53**, 1911 (2018).
22. R. Balen, W. V. da Costa, J. de Lara Andrade, J. F. Piai, E. C. Muniz, M. V. Companhoni, T. U. Nakamura, S. M. Lima, L. H. da Cunha Andrade, P. R. S. Bittencourt, A. A. W. Hechenleitner, E. A. G. Pineda and D. M. Fernandes, *Appl. Surf. Sci.*, **385**, 257 (2016).
23. M. Jamil, I. U. Haq, B. Mirza and M. Qayyum, *Ann. Clin. Microb. Anti.*, **11**, 11 (2012).
24. A. Naskar, H. Khan, R. Sarkar, S. Kumar, D. Halder and S. Jana, *Mater. Sci. Eng., C.*, **91**, 743 (2018).
25. R. Khoushika and D. Brindha, *Int. J. Appl. Pharm.*, **9**, 116 (2017).
26. P. Chuysinuan, P. Pavasant and P. Supaphol, *ACS Appl. Mater. Interfaces*, **4**, 3031 (2012).
27. T. Thanyacharoen, *J. Mol. Liq.*, **248**, 1065 (2017).
28. A. V. Lodha and P. S. Joshi, *J. Macromol. Sci. Part B*, **47**, 201 (2007).
29. S. Gurunathan, J. W. Han, A. Abdal Dayem, V. Eppakayala and J. H. Kim, *Int. J. Nanomedicine*, **7**, 5901 (2012).
30. A. W. Coats and J. P. Redfern, *Nature*, **964**, 68 (2011).
31. P. Ilangovan, M. S. Sakvai and A. B. Kottur, *Mater. Chem. Phys.*, **193**, 203 (2017).
32. Y. H. Leung, A. M. C. Ng, X. Xu, Z. Shen, L. A. Gethings, M. T. Wong, C. M. N. Chan, M. Y. Guo, Y. H. Ng and A. B. Djurišić, *Small*, **10**, 1171 (2014).
33. S. Mathew, J. Mathew and E. K. Radhakrishnan, *J. Polym. Res.*, **26**, 1 (2019).
34. C. Jayaseelan, A. A. Rahuman, G. Rajakumar, A. V. Kirthi, T. Santhoshkumar, S. Marimuthu, A. Bagavan, C. Kamaraj, A. A. Zahir and G. Elango, *Parasitol. Res.*, **109**, 185 (2011).
35. M. Bilal, Y. Zhao, T. Rasheed, I. Ahmed, S. T. S. Hassan, M. Z. Nawaz and H. M. N. Iqbal, *Int. J. Environ. Res. Public Health*, **16**, 598 (2019).
36. S. Hajji, R. B. S.-B. Salem and M. Hamdi, *Process Saf. Environ. Prot.*, **111**, 112 (2017).
37. R. Thaya, B. Malaikozhundan, S. Vijayakumar, J. Sivakamavalli, R. Jeyasekar, S. Shanthi, B. Vaseeharan, P. Ramasamy and A. Sonawane, *Microb. Pathog.*, **100**, 124 (2016).